



A limitation lifted: A conditional knockdown system reveals essential roles for Polo-like kinase and Aurora kinase 1 in *Trypanosoma cruzi* cell division

Justin Wiedeman^{a,b} , Ruby Harrison^{a,b} , and Ronald Drew Etheridge^{a,b,1}

Edited by Margaret Phillips, The University of Texas Southwestern Medical Center, Dallas, TX; received August 7, 2024; accepted December 20, 2024

While advances in genome editing technologies have simplified gene disruption in many organisms, the study of essential genes requires development of conditional disruption or knockdown systems that are not available in most organisms. Such is the case for *Trypanosoma cruzi*, a parasite that causes Chagas disease, a severely neglected tropical disease endemic to Latin America that is often fatal. Our knowledge of the identity of essential genes and their functions in *T. cruzi* has been severely constrained by historical challenges in very basic genetic manipulation and the absence of RNA interference machinery. Here, we describe the development and use of self-cleaving RNA sequences to conditionally regulate essential gene expression in *T. cruzi*. Using these tools, we identified essential roles for Polo-like and Aurora kinases in *T. cruzi* cell division, mirroring their functions in *Trypanosoma brucei*. Importantly, we demonstrate conditional knockdown of essential genes in intracellular amastigotes, the disease-causing stage of the parasite in its human host. This conditional knockdown system enables the efficient and scalable functional characterization of essential genes in *T. cruzi* and provides a framework for the development of conditional gene knockdown systems for other nonmodel organisms.

Trypanosoma cruzi | conditional knockdown | aptazyme | parasite | protozoan

Trypanosoma cruzi is a protozoan parasite responsible for Chagas disease in Latin America. Also known as American trypanosomiasis, Chagas disease is considered the most significant parasitic illness of the Western Hemisphere (1), currently infecting 6 to 7 million people and estimated to cause 12,000 deaths per year (2). *T. cruzi* is a dixenous kinetoplastid parasite transmitted via the feces of hematophagous triatomine insects (3). It alternates between actively dividing extracellular forms in the insect gut (epimastigotes) and intracellular forms in the vertebrate host (amastigotes). Transmission between hosts primarily occurs via nondividing infectious forms of the parasite known as trypomastigotes (4). Organisms of the kinetoplastid lineage such as *T. cruzi* are well known for an array of unusual biological processes distinct from traditional model eukaryotes, including editing of mitochondrial DNA transcripts (5), surface antigenic variation (6), polycistronic gene transcription (7), and complex life cycles (8, 9). Progress toward understanding cryptic elements of *T. cruzi* biology is tangible (10–15), yet slow when compared to advances made in other protozoans which benefit from better-developed molecular tools (16–21). Despite *T. cruzi* being actively studied for nearly 120 y (22), our understanding of the enigmatic biology and pathogenesis of this parasite remains limited, and fundamental questions regarding the genes necessary for essential processes such as proliferation, stage transition, host cell invasion, and host cell egress remain unanswered.

Our ability to identify and interrogate the function of essential genes in *T. cruzi* is crippled by the lack of effective genetic tools (23), and many common strategies used to study essential genes in other organisms are not applicable to *T. cruzi*. For example, bioinformatics cannot be used to reliably predict the function of most *T. cruzi* genes since 57 percent lack identifiable sequence similarity with annotated protein databases (24). RNA interference (RNAi), which has been used to great effect in the study of African trypanosomes (25), is unavailable as the essential RNAi processing machinery is absent in *T. cruzi* (26). Forward genetics screening tools used in haploid protozoans like apicomplexans [such as transposon-mediated mutagenesis (27) and genome-wide CRISPR/Cas9-mediated gene knockouts (19)] are impractical in *T. cruzi* since it is both diploid (28) and does not utilize nonhomologous end-joining to repair double-stranded DNA breaks. In contrast to many model organisms, *T. cruzi* employs a lesser-known alternative to the nonhomologous end-joining pathway called microhomology-mediated end joining (29, 30), which is both error-prone and has the potential to disrupt the coding sequence of adjacent genes in the chromosome during

Significance

Trypanosoma cruzi is a neglected protozoan parasite responsible for Chagas disease, the most significant parasitic illness in the Americas. Here, we present the development of the first conditional knockdown system to enable loss-of-function studies on essential genes in this organism. Our system uses a small-molecule-regulated self-cleaving RNA sequence placed downstream of the target gene, enabling the rapid depletion of both mRNA and protein. Using this tool, we induced knockdown of Polo-like kinase and Aurora kinase 1 and observed severe defects in proliferation and division in both the insect and mammalian life stages of the parasite. This conditional knockdown system offers a robust method to characterize essential genes and validate potential drug targets in this important human pathogen.

Author affiliations: ^aCenter for Tropical and Emerging Global Diseases, University of Georgia, Athens, GA 30602; and ^bDepartment of Cellular Biology, University of Georgia, Athens, GA 30602

Author contributions: J.W., R.H., and R.D.E. designed research; J.W. and R.H. performed research; J.W., R.H., and R.D.E. analyzed data; and J.W., R.H., and R.D.E. wrote the paper.

The authors declare no competing interest.

This article is a PNAS Direct Submission.

Copyright © 2025 the Author(s). Published by PNAS. This article is distributed under [Creative Commons Attribution-NonCommercial-NoDerivatives License 4.0 \(CC BY-NC-ND\)](#).

¹To whom correspondence may be addressed. Email: ronald.etheridge@uga.edu.

This article contains supporting information online at <https://www.pnas.org/lookup/suppl/doi:10.1073/pnas.2416009122/DCSupplemental>.

Published February 18, 2025.

the repair process. Promoter-based gene regulation (31) is also not feasible since trypanosomes lack individual promoters for most genes. Instead, they generate polycistronic transcripts which require cotranscriptional 5' trans-splicing and 3' polyadenylation to generate individual messenger RNAs (mRNA) for translation (reviewed in ref. 32). Historically, the direct deletion of target genes using homologous recombination and drug selection has been unreliable (29), although the adaptation of CRISPR/Cas9-based gene editing to *T. cruzi* vastly improved recombination efficiency (29, 33). Prior to the introduction of CRISPR/Cas9, virtually nothing was known of the “essential” genome, as only eleven genes [out of an estimated 12,000 total genes (34)] were classified as possibly essential (35). Even now, genes are still classified as putative-essential only if double knockouts do not survive transfection and selection, and their functions can only be evaluated in mixed populations in a short window between transfection and cell death (36–38). Thus, the study of essential genes in this parasite has improved only marginally with CRISPR/Cas9 (39). Ultimately, the absence of a conditional gene knockdown system has limited the in-depth study of *T. cruzi* (23, 39). Various attempts to develop conditional knockdown strategies have been reported, but none have enabled the study of essential genes (37, 38, 40–42). In this work, we report the successful use of a hammerhead ribozyme-based strategy to conditionally regulate expression of essential genes in *T. cruzi*.

Hammerhead ribozymes (HHRs) are self-cleaving RNA sequences present in all kingdoms of life (reviewed in ref. 43). In eukaryotes, they are thought to function in retrotransposon processing (44) and gene regulation (45). A HHR from the trematode *Schistosoma mansoni* (44) has been intensively studied and developed into various “aptazymes” (46) (also called “riboswitches”) where an RNA aptamer which binds to a ligand such as tetracycline (Tet) (47) or theophylline (Theo) (48) is fused to the ribozyme catalytic core. The resulting aptazyme allows regulation of RNA self-cleavage using an exogenous ligand. When incorporated into the untranslated regions (UTR) of target genes (i.e., “tagging”), aptazymes can conditionally regulate gene expression (49, 50). Here, we describe the development and validation of the Short Hammerhead Aptazyme-Regulated Knockdown (SHARK) system in *T. cruzi* using optimized *S. mansoni* hammerhead-based aptazymes inserted into endogenous gene loci. We identified three SHARK versions using different aptazymes which are functional in *T. cruzi*: one which induces knockdown by addition of Tet (51) (Shark1), one inducing knockdown by removal of Tet (50) (Shark2), and one that induces knockdown by addition of the caffeine analogue Theo (Shark3) (51). In order to validate the SHARK system as an effective tool to conduct loss-of-function studies, we have selected *T. cruzi* Polo-like kinase (PLK) and Aurora kinase B (AUK1) as model essential genes. PLK and AUK1 are two of the best-characterized kinases and are well known for their essential roles regulating cell division in both traditional model eukaryotes (reviewed in refs. 52 and 53) and trypanosomatids (54–57). Using SHARK, we demonstrate the effectiveness of this system in producing rapid and robust knockdown of PLK and AUK1, resulting in marked proliferation defects in both insect and mammalian stages of *T. cruzi*. We then functionally characterized the result of SHARK-mediated knockdown of both genes and identified roles for PLK and AUK1 in trypanosome cytokinesis and mitosis, respectively. The SHARK system, therefore, represents a simple and straightforward method to functionally characterize essential genes in *T. cruzi*.

Results

Development of an Aptazyme-Based Conditional Knockdown System for *T. cruzi*.

The activity of a HHR is heavily influenced by the intracellular context in which it is found (50, 58–60). As a result,

HHR-based aptazymes need to be empirically tested in organism-specific screens to assess functionality. To identify aptazymes able to conditionally regulate gene expression in *T. cruzi* epimastigotes, we screened a panel of aptazyme candidates (51) (*SI Appendix*, Fig. S1A) derived from the N79 *S. mansoni* HHR (61) that differed primarily in the composition of the communication module (CM) (46) sequences which link the HHR to the ligand-binding aptamer region (Fig. 1 A, Left). In this initial screen, we tagged two *T. cruzi* genes [Spef1 (TcYC6_0088120) and SUB2 (TcYC6_0021830)] in their 3' UTRs with different aptazymes and a 3x-Ty (referred to as -Ty) epitope tag and assessed tagged protein abundance before and after 48 or 72 h Tet treatment (*SI Appendix*, Fig. S1 B and C). All aptazymes reduced protein expression after Tet treatment, but differed significantly in the basal expression (gene expression in the absence of Tet) of tagged genes.

We reasoned that the basal expression of aptazyme-tagged genes was being influenced by background cleavage activity of the HHR in the absence of ligand and that maintaining robust basal expression was critical for homozygous aptazyme tagging of essential genes. In support of this, we observed that SUB2 and PLK (TcYC6_0047790), both predicted essential genes, could only be tagged at both loci with an inactive, or “dead,” version of an aptazyme (*SI Appendix*, Fig. S1D (schematic) and *SI Appendix*, Fig. S1E). This suggested that uninduced aptazyme cleavage was exerting negative selective pressure and, therefore, could prevent efficient homozygous tagging of essential genes. Thus we selected the aptazyme from our initial screen with the highest basal expression, Tc14 (51), and undertook PLK-guided HHR sequence optimization (Fig. 1 A, Right) to reduce background cleavage activity. We selected three bases in Stem 1 (S1) that influence hammerhead activity through interactions with adjacent bases in S1 and Loop 1 (L1) (61, 62) (Fig. 1 A, Right) and created single-base S1 mutants of Tc14 (e.g., U108G, C109A, and C110A). We then tagged both loci of PLK with the original and S1 Tc14 mutants and measured basal expression levels of PLK mRNA and protein.

In the absence of Tet, the original Tc14 reduced PLK transcript abundance by ~50% relative to Y-strain (parental) epimastigotes (*SI Appendix*, Fig. S1F), but PLK mRNA levels were restored to near normal levels (1.2× Y-strain) in the C110A mutant, while U108G and C109A mutants increased PLK mRNA levels above Y-strain (*SI Appendix*, Fig. S1F). PLK basal protein expression was likewise improved over the original Tc14 in the S1 mutants, as U108G, C109A, and C110A versions all increased protein expression by at least 2.4× (Fig. 1B, see -Tet). The frequency of homozygous aptazyme-tagged clones was also altered in the S1 mutants. Using PCR to genotype clonal PLK-Tc14 cell lines, we noted that the frequency of homozygous clones was increased in each of the S1 mutants compared to original Tc14 (*SI Appendix*, Fig. S1G). Finally, we investigated the effect of S1 mutations on Tc14 cleavage activity. After 72 h Tet treatment, C109A and C110A aptazymes decreased PLK protein abundance by 75% and 95%, respectively, but U108G-Tc14 was not active (Fig. 1B, see +Tet). Taken together, these data demonstrate that PLK basal expression is decreased by tagging with the original Tc14 aptazyme but can be restored by mutating Tc14 C110, without compromising robust Tet-inducible transcript cleavage and protein knockdown by the aptazyme. We therefore selected Tc14-C110A for future studies and renamed it Shark1.

PLK and AUK1 Are Essential for Epimastigote Proliferation.

After completing PLK-guided optimization of the Tc14 sequence, we selected and tagged another putative essential gene, AUK1 (TcYC6_0013480), with Shark1 [Fig. 1C (schematic)] as both PLK and AUK1 are essential in African trypanosomes and their functions have been well characterized (54, 56, 63–65). Given the

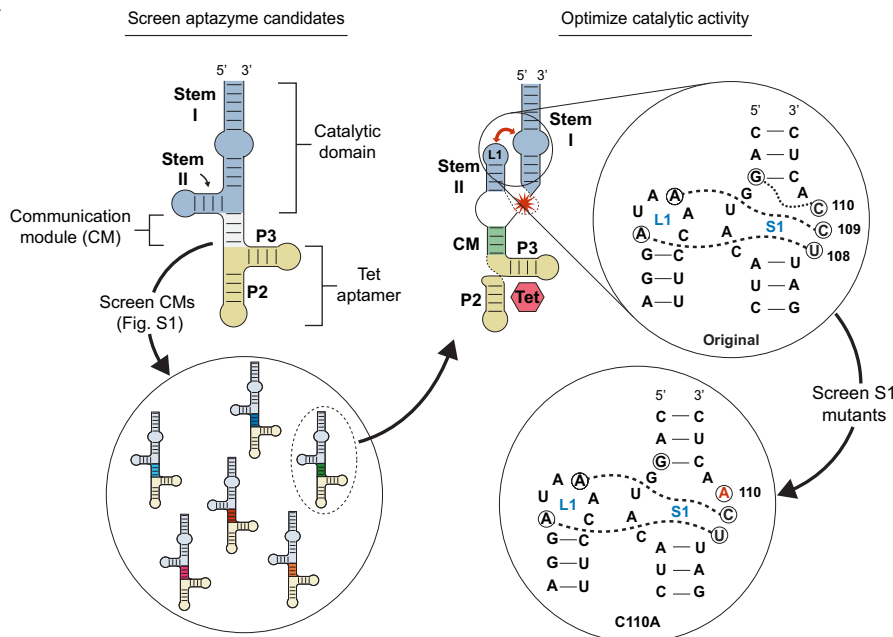
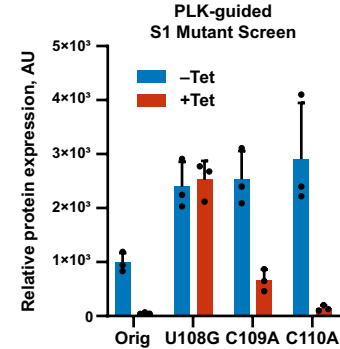
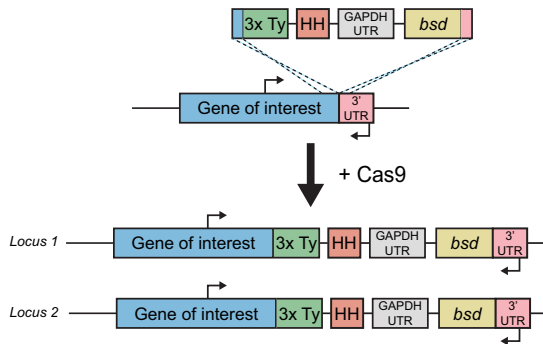
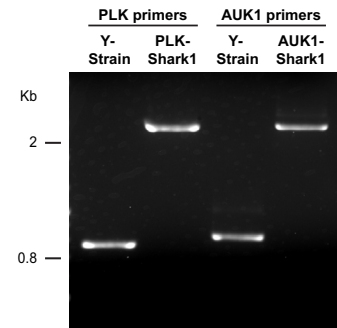
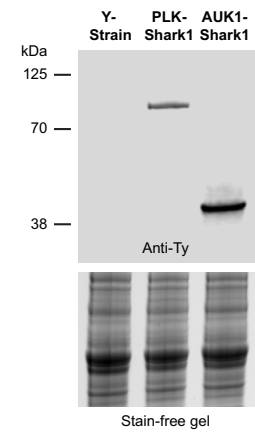
A**B****C****D****E**

Fig. 1. In vivo selection and optimization of a conditional Tet-responsive aptazyme epitope tag in *T. cruzi*. (A) Illustration of aptazyme components and in vivo screening and optimization workflow. (Left) An example aptazyme illustrated in the inactive conformation. Modules are labeled and color-coded. Stems I and II are labeled in the catalytic domain module. RNA aptamer stems P2 and P3 are labeled. Aptazyme candidates with different CM sequences were screened for basal expression levels of tagged genes by western blot (*SI Appendix*, Fig. S1). (Right) Illustration of Tc14, the top performing aptazyme candidate, in the active conformation induced by Tet binding. The red star indicates the approximate site of self-cleavage. The bidirectional red arrow illustrates the interaction between Loop 1 (L1) and Stem 1 (S1) after Tet binding by the RNA aptamer. Expanded circle illustrates specific interactions involving three bases in S1 (U108, C109, and C110, circled and labeled) important for stabilizing the ribozyme in the active conformation. Dotted lines connect bases in L1 and S1 where hydrogen bonding is likely to occur during catalysis. (B) Effect of S1 mutation on Tc14 activity. Tc14 S1 mutants were used to tag PLK, and protein basal expression and knockdown (induced by 5 µg/mL Tet for 72 h) were evaluated in epimastigotes by western blot. Anti-Ty signal was normalized to total protein content. The average of three replicates is presented. Error bars indicate SD. (C) Design of the PCR-generated cassette for Cas9-mediated incorporation of the Tc14-C110A (Shark1) aptazyme and 3x-Ty epitope tag into the 3' UTR of a gene of interest. PCR primer annealing sites flanking the recombination site are indicated with directional arrows. (D) Diagnostic PCR to identify homozygous epimastigote clones. Primers flanking the recombination site were used to differentiate between wild-type and recombinant loci. Representative PLK-Shark1 and AUK1-Shark1 clonal cell lines are compared to Y-strain (parental) trypanosomes. (E) Expression of 3x-Ty Shark1-tagged PLK and AUK1 genes in representative clonal epimastigotes lines confirmed by western blot. PLK-3x-Ty predicted MW = 85 kDa. AUK1-3x-Ty predicted MW = 38.9 kDa. Stain-free gel illustrates total protein loading before transfer.

high conservation of both kinase sequences in *T. cruzi* and their likely involvement in similar essential functions, we hypothesized that PLK and AUK1 could serve as reliable model genes to evaluate the efficacy of the SHARK system in conducting loss-of-function studies in this parasite. Homozygous clonal cell lines of PLK-Shark1 and AUK1-Shark1 were selected for further study after genotyping (Fig. 1D) and confirming expression of PLK-Ty and AUK1-Ty by western blot (Fig. 1E) and immunofluorescence (*SI Appendix*, Fig. S2). To test whether Shark1 could be used to functionally characterize essential genes, we first investigated gene knockdown kinetics and specificity with PLK and AUK1. We treated Shark1-tagged epimastigotes with Tet to induce gene knockdown [Fig. 2A (schematic)] and tracked

protein expression (Fig. 2 B and E, Left, quantified in Right) and transcript abundance (Fig. 2 C and F) over time. Aptazyme activation decreased PLK and AUK1 protein levels by 92% and 80% after 24 h (Fig. 2 B and E, Right), and decreased mRNA abundance by 85% and ~90%, respectively, after 120 min (Fig. 2 C and F). Since trypanosomes carry out polycistronic transcription [followed by trans-splicing and polyadenylation to produce mature transcripts (schematic in *SI Appendix*, Fig. S3A) (reviewed in ref. 32)], we considered the possibility that incorporation of an aptazyme might impact adjacent genes transcribed on the same polycistron. To test this, we treated PLK-Shark1- and AUK1-Shark1-tagged epimastigotes with Tet and measured the mRNA abundance of genes

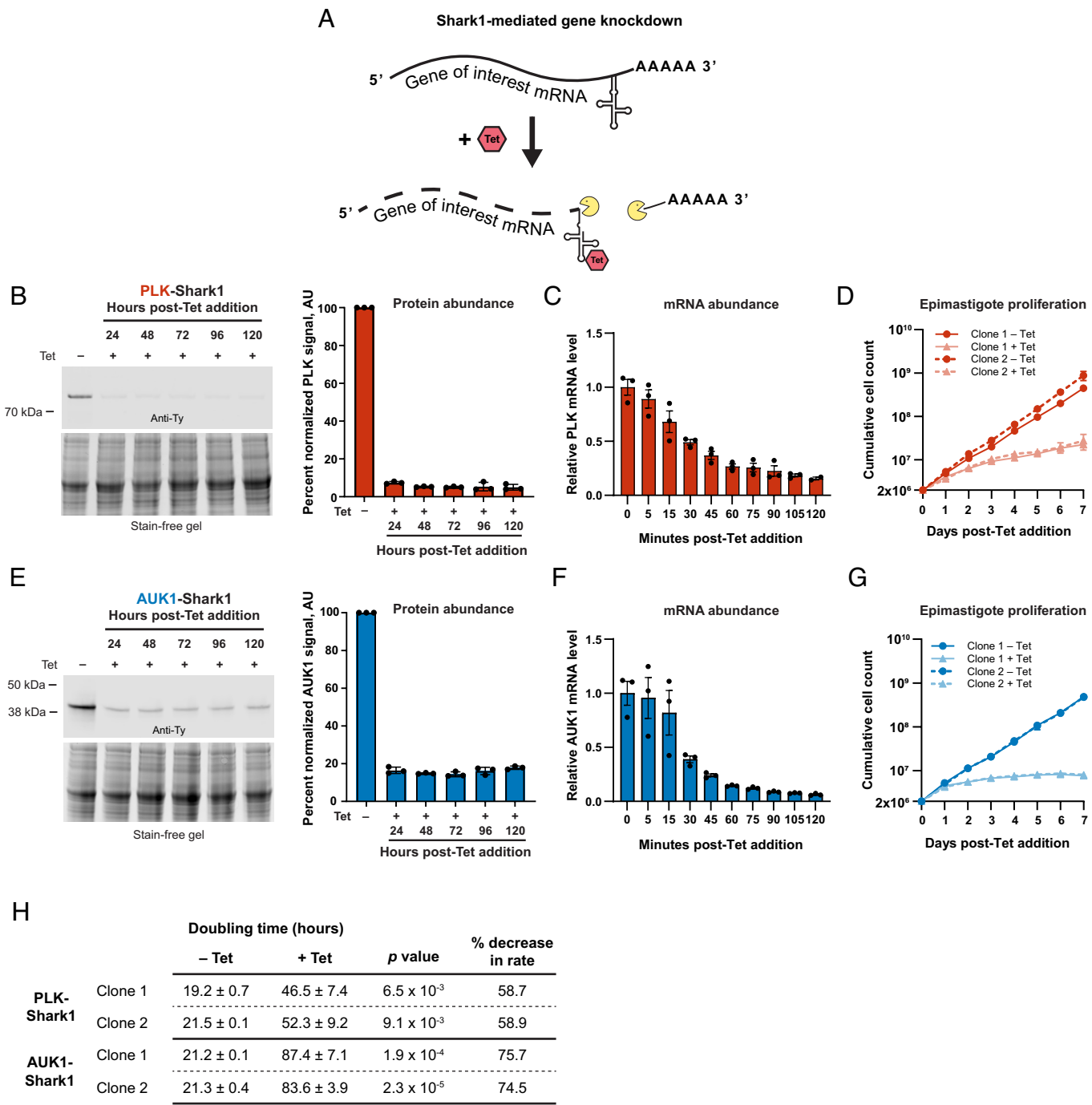


Fig. 2. PLK and AUK1 are essential for epi-mastigote proliferation. (A) Illustration of mRNA degradation after Tet-induced aptazyme cleavage. (B–D), PLK analysis. (E–G), AUK1 analysis. (B and E) (Left) Representative western blots illustrating the effect of Tet on PLK-Shark1-3x-Ty (B) and AUK1-Shark1-3x-Ty (E) abundance. Epi-mastigotes were treated with Tet (5 µg/mL) and incubated at 28 °C for the indicated times and processed for western blotting with an anti-Ty antibody. Stain-free gel indicates protein loading before transfer to the membrane. (Right) PLK and AUK1 signal was measured, normalized to total protein content, and plotted as the average percent signal of an untreated control. AU = arbitrary units. Error bars represent SD. (C and F) Effect of Tet treatment on PLK and AUK1 mRNA abundance. Epi-mastigotes were treated with 5 µg/mL Tet at 28 °C and collected at the indicated time points for quantitative reverse-transcriptase PCR. PLK (C) and AUK1 (F) expression was normalized to the reference gene actin 1 and compared to uninduced controls. Error bars show SD. (D and G) Proliferation time course after PLK (D) and AUK1 (G) knockdown. Epi-mastigotes from two clonal lines seeded at a density of 2×10^6 /mL were incubated for 7 d ± 5 µg/mL Tet at 28 °C. Cell density was measured each day using a Beckman Coulter Counter and diluted periodically with fresh media (±Tet) to maintain log-phase growth. The average cumulative cell density at each time point from three independent experiments is presented. Error bars represent SD. (H) Effect of 5 µg/mL Tet on population doubling times (± 1 SD) in hours. Data from three replicates were analyzed. Rates between –Tet and +Tet samples were compared and P values obtained using Student's t test.

immediately up and downstream of the PLK and AUK1 coding sequences. Knockdown of PLK and AUK1 did not decrease adjacent gene transcript levels in short (*SI Appendix*, Fig. S3 B and D) or extended (*SI Appendix*, Fig. S3 C and E) time course experiments, while target transcript levels were reduced by at least 90% after 24 h. We conclude that aptazyme suppression of gene expression is rapid

and specific, without decreasing transcript abundance of neighboring genes. Next, we assessed the effect of PLK and AUK1 knockdown on epi-mastigote proliferation. We knocked down gene expression and monitored cell growth over 7 d in two clonal PLK-Shark1 and AUK1-Shark1 cell lines (Fig. 2 D and G). Knockdown of either gene dramatically reduced proliferation, as PLK knockdown slowed

proliferation by ~60% and AUK1 knockdown slowed proliferation by ~75% (Fig. 2*H*), while Tet alone had no effect on Y-strain epimastigote proliferation (*SI Appendix*, Fig. S4 *A* and *B*). In the absence of Tet, Shark1-tagged PLK and AUK1 clones demonstrated a minor increase in the average doubling time (20.8 h) relative to the parental Y-strain (18.6 h) (Fig. 2*H* and *SI Appendix*, Fig. S4*B*). We conclude that PLK and AUK1 are essential for proliferation in *T. cruzi* epimastigotes.

PLK Promotes Symmetric Cytokinesis in Epimastigotes. In model eukaryotes, PLK regulates progression through the cell division cycle by promoting mitosis and cytokinesis (52). In African trypanosomes, PLK knockdown impacts cytokinesis but not mitosis (56). To determine whether PLK regulates cytokinesis or mitosis in *T. cruzi* epimastigotes, we induced PLK knockdown and stained trypanosomes with the fixable plasma membrane dye mCLING (66) and Hoechst. We evaluated the kinetoplast (K) (an organelle containing the condensed mitochondrial genome, reviewed in ref. 67) and nucleus (N) configurations of individual cells, since defects in the cell division cycle in kinetoplastids can be detected by abnormal K/N configurations (for a review of the trypanosome cell division cycle, see ref. 68). Briefly, a trypanosome in G1 contains 1K1N. During the S-phase, the kinetoplast replicates and divides to produce a 2K1N cell, which performs mitosis to form a 2K2N

trypanosome. Following mitosis, a 2K2N trypanosome undergoes cytokinesis to produce two daughter 1K1N cells.

Uninduced PLK-Shark1 trypanosomes progressed through mitosis and cytokinesis normally (Fig. 3 *A*, *Top row*), dividing into two 1K1N daughter cells after properly partitioning kinetoplasts and nuclei along a central cleavage plane. PLK knockdown, however, produced unusual cellular morphologies during cytokinesis, as the nuclei failed to properly segregate on opposite sides of the cleavage plane, producing daughter cells with either two nuclei (1K2N) or no nuclei (1K0N) (Fig. 3 *A*, *Bottom row*). Daughter cells with normal (1K1N) configurations decreased by 73% and cells with “abnormal” K/N configurations became the dominant population (71.6% of all cells) over the course of the experiment (Fig. 3 *B*). After 24 h of knockdown, postmitotic 2K2N trypanosomes increased in abundance nearly 500% (Fig. 3 *B*), and 1K2N and 1K0N trypanosomes began to accumulate (Fig. 3 *C*), consistent with both delayed and asymmetric cytokinesis (69, 70). By 72 h, cells with complex K/N phenotypes ($xKxN$, where $x > 2$) became the predominant cell type in culture (Fig. 3 *C*), likely the product of multiple rounds of kinetoplast replication, mitosis, and aberrant cytokinesis. In contrast, 72 h Tet treatment had no effect on Y-strain epimastigote K/N configuration (*SI Appendix*, Fig. S4*C*). The abnormal K/N phenotypes we observed after PLK knockdown are consistent with RNAi-based data from *T. brucei* (56), highlighting the efficacy of

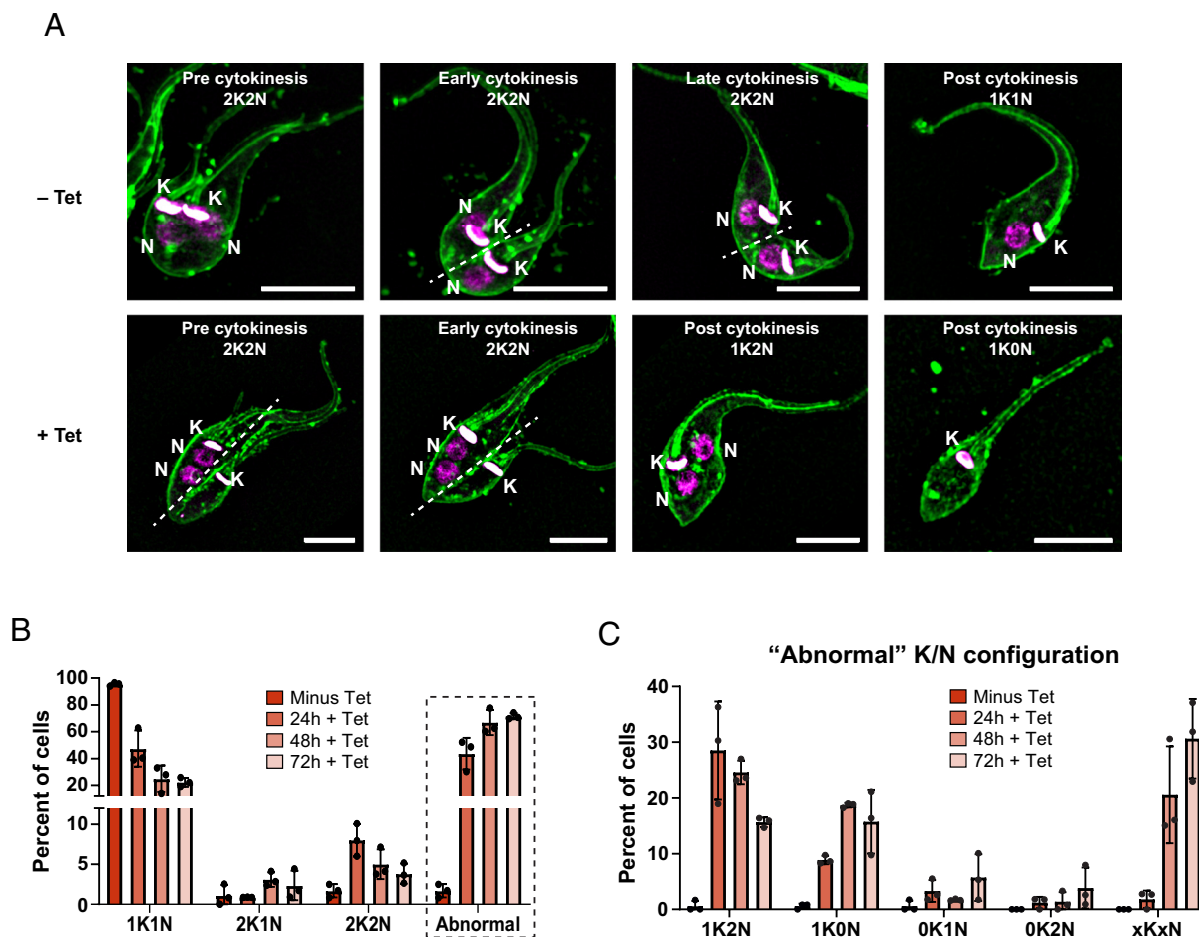


Fig. 3. PLK is essential for symmetric cytokinesis in epimastigotes. PLK-Shark1 epimastigotes treated with Tet (5 μ g/mL) for 24, 48, or 72 h were collected at the indicated time points and stained with mCLING (66) and Hoechst 33342 for microscopic analysis. (A) Example images of trypanosomes before (*Top*) or after (*Bottom*) PLK knockdown. The *Top row* illustrates the typical configuration of kinetoplasts (K) and nuclei (N) in an epimastigote during cytokinesis. The *Bottom row* highlights trypanosomes with abnormal kinetoplast and nucleus arrangements before, during, and after cytokinesis. The cytokinesis stage and kinetoplast/nucleus configuration of each cell are indicated in each panel. The dashed white line indicates the division plane. (Scale bars, 5 μ m.) (B) The number of kinetoplasts and nuclei per cell was determined. The average percent of cells with different K/N configurations from three independent experiments is presented. N > 150 per replicate. (C) Specific K/N configurations comprising the “Abnormal” population from panel B. $xKxN = >2K$ or $>2N$.

the SHARK knockdown system and indicating that PLK plays similar roles in both trypanosome species. We conclude that PLK is essential for symmetric cytokinesis in *T. cruzi* epimastigotes.

AUK1 Regulates Mitosis in Epimastigotes. AUK1 plays an important role regulating chromosome segregation during mitosis in a wide range of eukaryotes (reviewed in ref. 71) and in *T. brucei* (54, 63). Prior studies in *T. cruzi* have shown that AUK1 overexpression produces a mild defect in proliferation and delays completion of mitosis (72), but no loss-of-function studies have been reported. We hypothesized that AUK1 is essential for mitosis in *T. cruzi* as in other eukaryotes. Having previously shown that knockdown of AUK1 severely impacts epimastigote proliferation (Fig. 2 G and H), we examined the cellular morphology in AUK1-depleted epimastigotes stained with mCLING and Hoechst for abnormalities that could explain this growth defect. As expected, uninduced (−Tet) trypanosomes performed normal mitosis, equally dividing the nucleus before ingress of the cleavage furrow (73) (Fig. 4 A, Top row). AUK1 knockdown delayed or inhibited mitosis, but cytokinesis still occurred, producing trypanosomes with abnormally shaped nuclei that were unequally divided between daughter cells (Fig. 4 A, Bottom row). Quantitation of kinetoplasts and nuclei revealed a 300% increase in premitotic (e.g., 2K1N) cells and a 70% decrease in postmitotic 2K2N cells after 24 h, suggesting inhibition of mitosis (Fig. 4B). Trypanosomes without a nucleus (e.g., 1K0N) also appeared, eventually comprising 30% of all cells (Fig. 4B). Although possessing a seemingly normal K/N configuration, many of the 1K1N trypanosomes had abnormally sized nuclei after AUK1 knockdown. We measured the nuclear area of 1K1N trypanosomes and found that 47% of nuclei were abnormally sized (both larger and smaller as compared to untreated Y-strain), with the mean area increasing from 1.9 to 2.6 μm^2 after 72 h of knockdown (Fig. 4 C and D). Interestingly, 72 h Tet treatment of Y-strain decreased the mean nucleus area 10%, from 2.1 to 1.9 μm^2 (Fig. 4D and SI Appendix, Fig. S4D). The biological relevance of this finding is unclear, since Tet treatment did not slow proliferation of Y-strain epimastigotes or affect K/N configuration (SI Appendix, Fig. S4A and C). Thus, knockdown of AUK1 reveals its essential role in mitosis in *T. cruzi* epimastigotes, reflecting an analogous phenotype observed in insect-stage *T. brucei* RNAi-based studies (74).

PLK and AUK1 Are Essential for Amastigote Proliferation. Intracellular *T. cruzi* amastigotes proliferate in infected host tissues and are responsible for the pathology associated with Chagas disease (75). To investigate whether Shark1 could be used to study essential genes in intracellular parasites, we studied the effects of Tet on PLK and AUK1 protein levels in aptazyme-tagged amastigotes colonizing vertebrate cells. Surprisingly, we found that gene knockdown was less efficient in amastigotes incubated at 37 °C (SI Appendix, Fig. S5) than it was in epimastigotes maintained at 28 °C (Fig. 2 B and E), a phenomenon that could be caused by the C110A mutation in S1 (76). Decreasing the amastigote incubation temperature from 37 °C to 28 °C after Tet addition improved knockdown efficiency, resulting in a 90% reduction in PLK and an 86% decrease in AUK1 expression (Fig. 5 A and D). To determine whether PLK or AUK1 are essential for proliferation, we infected a cardiomyocyte cell line (H9C2) (77, 78) with PLK-Shark1 or AUK1-Shark1 tryptomastigotes for 24 h at 37 °C, then removed extracellular trypanosomes and induced knockdown with Tet. Both the uninduced control and Tet-treated sample were then incubated at 28 °C for 72 h, and the number of amastigotes per cell was determined by fluorescence microscopy (Fig. 5 B and E). Knockdown of either gene inhibited amastigote proliferation, decreasing the median number of amastigotes per infected cell from 10 to 5 in PLK-Shark1 cells (Fig. 5C) and from

10 to 3 in AUK1-Shark1 cells (Fig. 5F). We also observed that Tet alone did not significantly affect Y-strain amastigote proliferation (SI Appendix, Fig. S6 A and B). We conclude that Shark1 can efficiently regulate *T. cruzi* gene expression in intracellular amastigotes and that PLK and AUK1 are essential for amastigote proliferation in infected host cells.

PLK Is Essential for Symmetric Cytokinesis in Amastigotes. Since we previously observed that PLK knockdown resulted in asymmetric cytokinesis in epimastigotes (Fig. 3), we next tested whether PLK also contributes to cytokinesis in amastigotes. Using the uninduced PLK-Shark1 line as a control, we induced knockdown for 72 h and examined intracellular parasites by fluorescence microscopy (Fig. 6A). While the uninduced (−Tet) amastigotes were morphologically normal (Fig. 6 A, Top row), knockdown of PLK (+Tet) produced trypanosomes with abnormal K/N configurations (Fig. 6 A, Middle and Bottom rows). As with epimastigotes, the 1K1N population decreased dramatically, from 95 to 32% of all cells (Fig. 6B). Amastigotes presenting as 1K ≥ 2N and 1K0N, phenotypes consistent with asymmetric cytokinesis (69, 70), comprised 49% of all cells (Fig. 6B). Tet had no effect on the K/N configuration of Y-strain amastigotes (SI Appendix, Fig. S6 C and D). We conclude that PLK is essential for symmetric cytokinesis in the amastigote form of *T. cruzi*.

AUK1 Is Essential for Symmetric Mitosis in Amastigotes. We hypothesized that as in epimastigotes (Fig. 4), AUK1 may be important for mitosis in amastigotes. To test this, we induced AUK1 knockdown for 72 h and assessed amastigote morphology (Fig. 7A). Uninduced AUK1-Shark1 amastigotes appeared normal (Fig. 7 A, Top row), but following knockdown, we observed amastigotes without nuclei and others with abnormally sized nuclei (Fig. 7 A, Middle and Bottom rows). The abundance of premitotic 2K1N cells increased 136% while postmitotic 2K2N cells decreased by 87% (Fig. 7B), and anucleate (1K0N) trypanosomes arose, comprising 17% of the population (Fig. 7B). Together, these data indicate that AUK1 depletion inhibits mitosis. As with epimastigotes, while the abundance of 1K1N amastigotes decreased only modestly, from 96 to 77% of all cells, many of these trypanosomes possessed abnormally sized nuclei (Fig. 7 A, Middle and Bottom rows). We measured the nucleus area in 1K1N amastigotes (Fig. 7C) and found that 47% of nuclei were abnormally large or small (compared to the untreated Y-strain), with the mean area increasing from 3.1 to 3.7 μm^2 (Fig. 7D). As with Y-strain epimastigotes, Tet treatment also decreased mean Y-strain amastigote nucleus area, from 3.1 to 2.6 μm^2 (Fig. 7D and SI Appendix, Fig. S6E). These data demonstrate that AUK1 is necessary for mitosis in the amastigote life stage of the parasite.

Alternative SHARK Versions. In our initial screens of aptazyme candidates, we found two additional HHR-based aptazymes capable of conditional gene knockdown in *T. cruzi*: one inducing knockdown in the absence of Tet (49, 50), which we called Shark2, and one inducing knockdown after treatment with the caffeine analog Theo (48), which we called Shark3. Unlike Shark1, which is activated by Tet, Shark2 is inhibited by Tet (see schematic in SI Appendix, Fig. S7A). Shark2 is considered a “Tet-ON” version since incubation with Tet turns on expression of genes regulated by the aptazyme. We incorporated Shark2 and a 3x-Ty tag into the PLK 3' UTR in the presence of Tet and evaluated two clonal cell lines. After Tet washout, PLK protein abundance decreased nearly 90% by day 4 postwashout (SI Appendix, Fig. S7 B and C) and epimastigote proliferation was inhibited (SI Appendix, Fig. S7D). In two clonal PLK-Shark2-1x-Ty lines, Tet washout inhibited

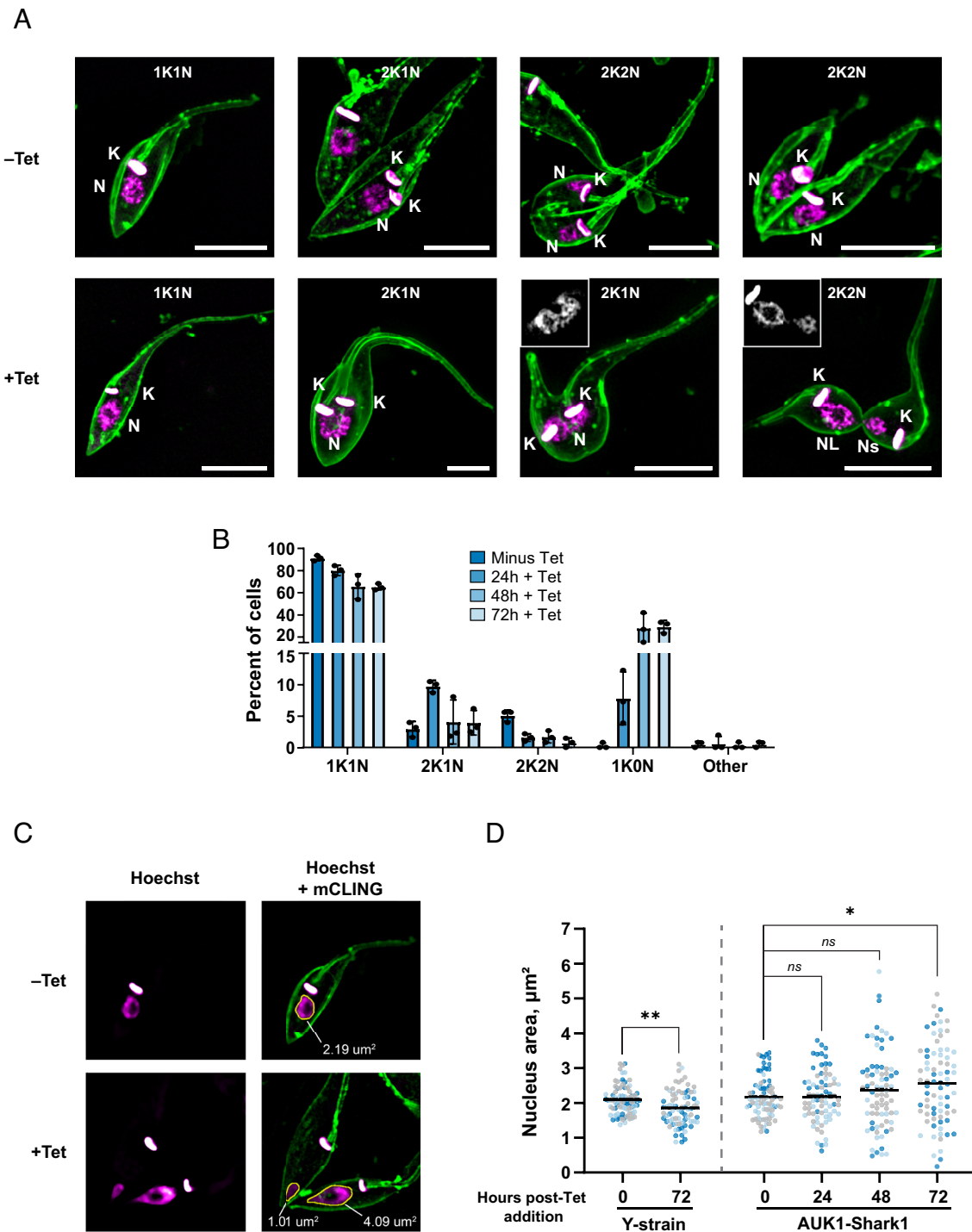


Fig. 4. AUK1 is essential for symmetric mitosis in epimastigotes. AUK1-Shark1 epimastigotes were incubated $\pm 5 \mu\text{g}/\text{mL}$ Tet at 28 °C and collected after 24, 48, or 72 h. Cells were stained with mCLING and Hoechst 33342 prior to microscopic analysis. (A) Representative images of epimastigotes before ($-$ Tet, Top row) and after ($+$ Tet, Bottom row) AUK1 knockdown. Control epimastigotes demonstrating typical numbers and positioning of kinetoplasts (K) and nuclei (N) during the cell division cycle are shown. An S-phase nucleus is visible in a 2K1N cell (Top row, Middle-Left) and after mitosis two nuclei are visible on opposite sides of a cleavage furrow in a 2K2N epimastigote before (Top row, Middle-Right) and after (Top row, Far-Right) initiation of cytokinesis. In $+$ Tet epimastigotes, a pictured 2K1N cell has not completed mitosis but cytokinesis has already been initiated (Bottom row, Middle-Right). The grayscale Inset shows a single-plane image of the Hoechst-stained nucleus. Unequally sized nuclei are present in a 2K2N cell that has nearly completed cytokinesis (Bottom row, far Right). The grayscale Inset shows a single-plane image of the Hoechst-stained nuclei. The K/N configuration of each cell is included in each panel. K = Kinetoplast, N = Nucleus, Ns = small nucleus, NL = large nucleus. (Scale bars, 5 μm .) (B) The number of K and N per cell was determined after AUK1 knockdown at the indicated time points. The average percent of cells with different K/N configurations is presented. N > 150 trypanosomes counted in each of three replicates. “Other” includes 1K2N, 0K1N, and $>2K > 2N$ cells. (C) Example images of nucleus size in 1K1N cells before and after AUK1 knockdown. The nucleus area in 1K1N epimastigotes was measured using ImageJ. A median filter was applied to each image to smooth the periphery of the nucleus and aid in automated detection. (D) Nucleus area measurements in Y-strain (parental) and AUK1-Shark1 epimastigotes. Data points are color-coded according to replicate number. Twenty-five 1K1N trypanosomes were evaluated in each of three replicates. A Mann–Whitney *U* test was performed to test for statistical significance between samples. For Y-strain 0 h vs. 72 h, $P = 1.8 \times 10^{-3}$; for AUK1-Shark1 0 h vs. 24 h, $P = 0.798$; for AUK1-Shark1 0 h vs. 48 h, $P = 0.380$; for AUK1-Shark1 0 h vs. 72 h, $P = 0.034$.

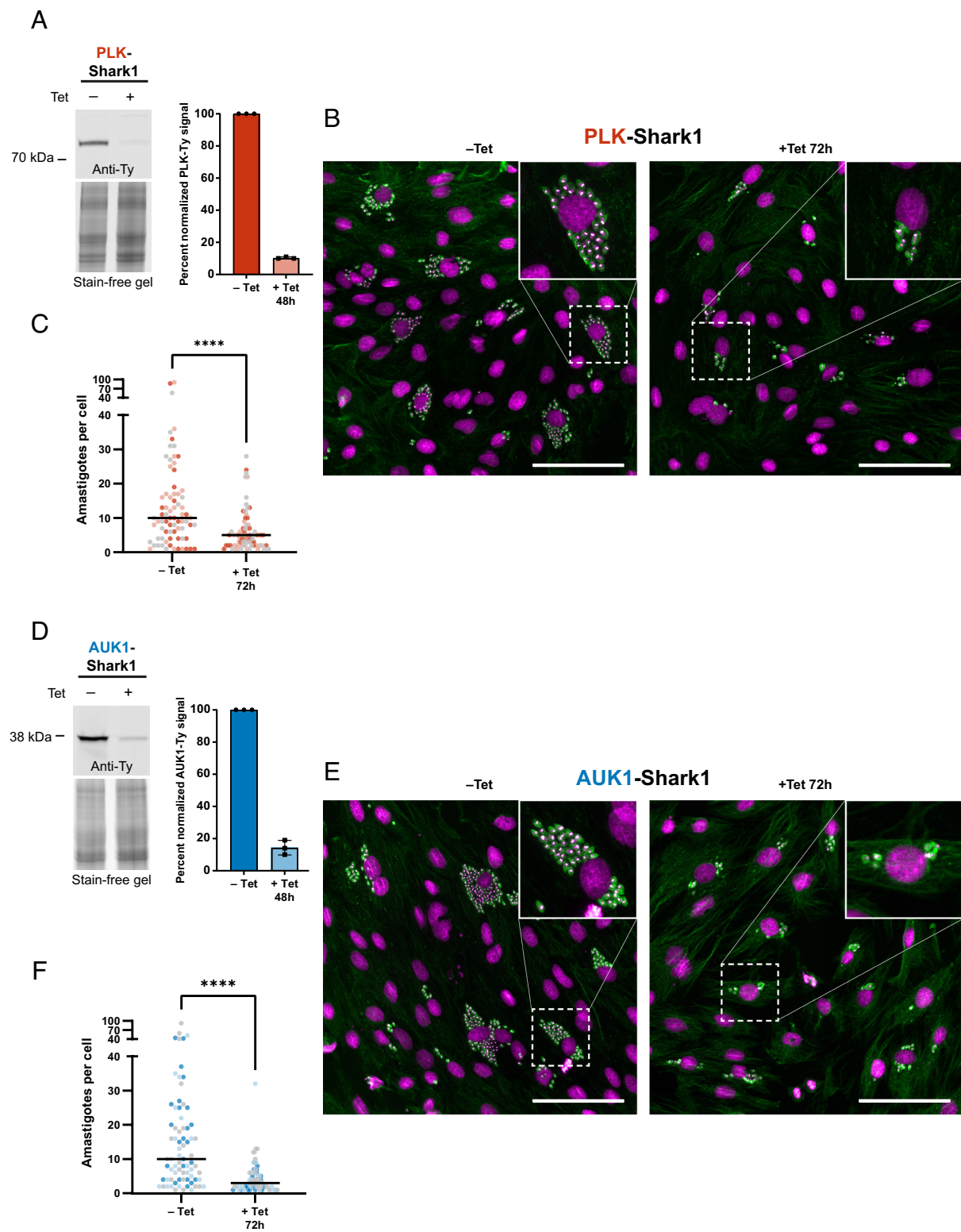


Fig. 5. PLK and AUK1 are essential for amastigote proliferation. (A–C) PLK analysis. (D–F) AUK1 analysis. (A and D) Tissue culture-derived PLK-Shark1 (A) and AUK1-Shark1 (D) trypanomastigotes were used to infect human foreskin fibroblasts (HFFs) for 96 h at 37 °C. Trypanomastigotes were washed off and HFF cells were incubated ±5 µg/mL Tet for 48 h at 28 °C. HFF cells were harvested from the tissue culture flask and intracellular amastigotes were released. Host cell debris was removed by filtration and filtered amastigotes were pelleted and subjected to SDS-PAGE and western blot. (Left) Representative western blot showing the effect of Tet on PLK-Ty (A) and AUK1-Ty (D) abundance. Anti-Ty signal was normalized to total protein loading, as determined by stain-free gel. PLK-3x-Ty predicted MW = 85 kDa, AUK1-3x-Ty predicted MW = 38.9 kDa. (Right) Average percent normalized PLK and AUK1 signal before and after knockdown from three biological replicates. Error bars represent SD. (B and E) Representative images of infected cardiomyocytes. Rat cardiomyocytes (H9C2) adhered to glass coverslips were infected with tissue culture-derived trypanomastigotes for 24 h at 37 °C. Trypanosomes were washed off and H9C2 cells were incubated ±5 µg/mL Tet for 72 h at 28 °C. Cells were fixed and stained with anti-trypanosome alpha-tubulin 1 (TAT1) antibody and DAPI. Image grids were captured and a gamma correction (0.7) was applied to the DAPI channel to aid in visualization of the trypanosome nucleus. Scale bars indicate 100 µm. (C and F) Amastigotes per cell before and after PLK (C) or AUK1 (F) knockdown. Data points are color-coded according to the replicate. Lines indicate the median number of amastigotes per infected cell (PLK – Tet = 10, PLK + Tet = 5; AUK1 – Tet = 10, AUK1 + Tet = 3). Twenty-five infected cells were evaluated in each replicate. Statistical significance of the difference in distribution of data points between –Tet and +Tet samples was assessed using a Mann–Whitney *U* test (For PLK *P* = 0.001 and for AUK1 *P* = 0.0001).

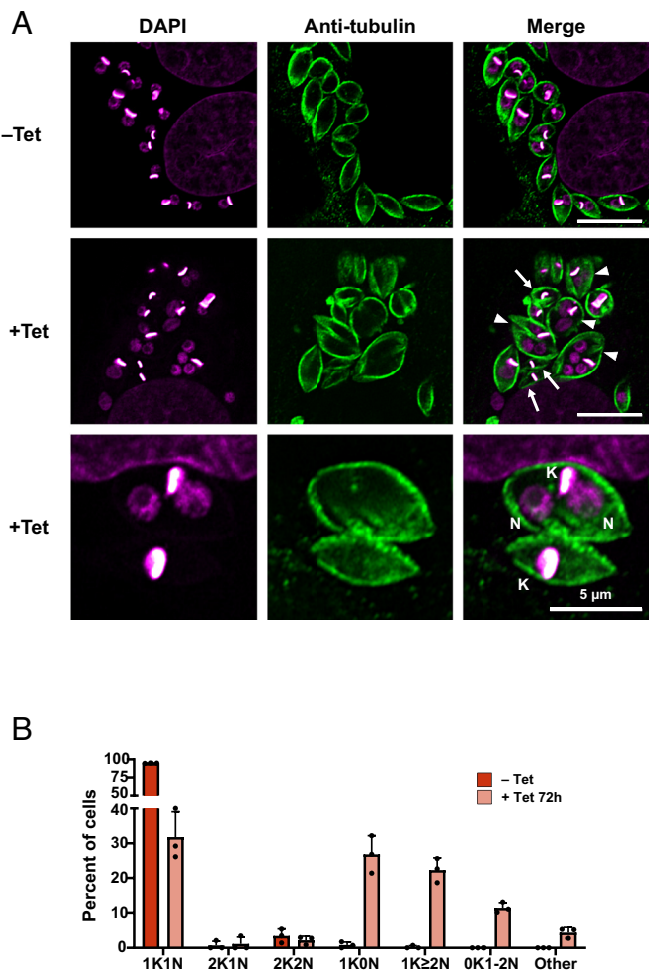


Fig. 6. PLK is essential for normal cytokinesis in amastigotes. PLK-Shark1 tissue culture-derived trypomastigotes were used to infect rat cardiomyocytes (H9C2) adhered to glass coverslips for 24 h at 37 °C. H9C2 cells were washed to remove trypanosomes and then incubated ±Tet (5 µg/mL) for 72 h at 28 °C. Cells were fixed and stained with TAT1 antibody and DAPI. (A) Example images of amastigotes. The Top row illustrates untreated amastigotes. The Middle row displays amastigotes with abnormal K/N configurations. Arrowheads indicate trypanosomes with 1 kinetoplast and ≥2 nuclei. Arrows indicate trypanosomes without a nucleus. Scale bars for Top and Middle rows = 10 µm. The Bottom row shows an enlarged image of a 1K2N and 1K0N amastigote. (Scale bar, 5 µm.) (B) The number of K and N per amastigote. N ≥ 100 amastigotes from at least five infected host cells per replicate. Three replicates were performed. The average percent K/N configuration type is presented. Other includes 2K > 2N, 0K > 2N, and 3K1N cell types.

proliferation (*SI Appendix*, Fig. S7E) and produced abnormal K/N configurations (1K2N and 1K0N) consistent with defects in cytokinesis (*SI Appendix*, Fig. S7 F–J). To create Shark3, we made a C88A mutant version (equivalent to C110A) of the Theo-responsive aptazyme Theo3 (51) as we did with Tc14 (Fig. 1 A and B). We then tagged PLK at its 3' UTR with Shark3 and a 3x-Ty tag and isolated clonal homozygous cell lines. Theo treatment reduced PLK protein levels by 80% in a time course experiment (*SI Appendix*, Fig. S8A) and inhibited epimastigote proliferation in two clonal PLK-Shark3 lines (*SI Appendix*, Fig. S8 B and C), without affecting Y-strain proliferation (*SI Appendix*, Fig. S4 A and B). Shark3-mediated knockdown of PLK induced asymmetric cytokinesis (*SI Appendix*, Fig. S8D), simultaneously producing 1K2N and 1K0N epimastigotes (*SI Appendix*, Fig. S8 E and F). Knockdown of PLK with Shark2 or Shark3 mirrored the effects of Shark1-mediated PLK knockdown in epimastigotes (Fig. 3), demonstrating their usefulness as alternative tools to functionally characterize essential genes in this organism.

Discussion

In this study, we developed an aptazyme-based platform (called SHARK) that facilitates the conditional knockdown of essential genes in the American trypanosome, *T. cruzi*. We first screened a panel of aptazymes (44, 51, 61) and identified three candidates [Shark1-3 (summarized in *SI Appendix*, Fig. S9 A–D, with the overall SHARK tagging strategy summarized in *SI Appendix*, Fig. S9E)] that enabled the regulation of endogenous gene expression. We then used site-directed mutagenesis to fine-tune the aptazyme activity of Shark1 and Shark3 to ensure both efficient tagging of essential genes at their genomic loci and robust and regulatable gene knockdown. Finally, we demonstrated the ability of all three SHARK aptazymes to regulate expression of essential genes. SHARK-mediated knockdown of essential genes is rapid, specific, and functional in both epimastigote and amastigote life cycle stages.

In order to demonstrate the efficacy of the SHARK conditional knockdown platform, we characterized the protein kinases PLK and AUK1 and identified essential roles for them in cytokinesis and mitosis, respectively. Morphological abnormalities caused by knockdown of these kinases were similar to findings in *T. brucei*, indicating conserved roles in *T. cruzi* and validating our system. PLK knockdown in *T. cruzi* produces abnormal phenotypes suggestive of asymmetric cytokinesis, likely caused by either improper positioning of organelles prior to ingression of the cleavage furrow (56, 79) or misplacement of the furrow itself (80). The localization of N-terminal epitope-tagged PLK in *T. cruzi* was also recently reported (12), and similar to those authors, we observed an increase in epitope-tagged PLK expression during S-phase, but the intracellular pattern appeared more diffuse, possibly resulting from the difference in epitope-tag placement. The phenotypes resulting from AUK1 knockdown are suggestive of aberrant chromosome segregation and mirror those of other model eukaryotes (63). As in insect-stage *T. brucei*, AUK1 knockdown inhibited mitosis but not cytokinesis (81–83), suggesting that *T. cruzi* lacks a checkpoint control mechanism to prevent cytokinesis if mitosis fails. Interestingly, in mammalian-stage *T. cruzi*, AUK1 knockdown did not inhibit cytokinesis, whereas in mammalian-stage *T. brucei*, AUK1 knockdown inhibits cytokinesis initiation (57, 63, 65). This suggests that while AUK1 operates in a similar fashion in the insect stages of both *T. cruzi* and *T. brucei*, there is an important divergence in the regulation of cell division between the mammalian stages of these parasites.

The SHARK platform represents a significant leap forward in our ability to conduct reverse genetics in *T. cruzi*. Nevertheless, some limitations of this system exist. Our tagging strategy places the glyceraldehyde phosphate dehydrogenase (GAPDH) intergenic region (84) immediately after the target gene to ensure proper polyadenylation and facilitate trans-splicing of the downstream antibiotic resistance gene. While the GAPDH UTR generally promotes robust gene expression, for some targets this may result in either over- or underexpression of tagged loci. Nearly all genes we have tested so far could be tagged at both genomic loci with an active SHARK tag. However, we found that some targets, like SUB2, can only be tagged at both loci with an inactive, or catalytically dead, aptazyme. Based on our quantification of SHARK-tagged PLK mRNA levels, we suspect that the insertion of an active aptazyme alone can have a minor impact on the basal expression of a target gene and can lead to subtle decreases in the growth rate in resulting cell lines. While this change appears to be tolerated in most cases, there will no doubt be loci where even minor changes in expression due to “leaky” knockdown could be detrimental. Additionally, *T. cruzi* possesses large gene families (34) that cannot practically be studied by incorporating an aptazyme into every locus of each gene copy. While we regard the current iteration of the

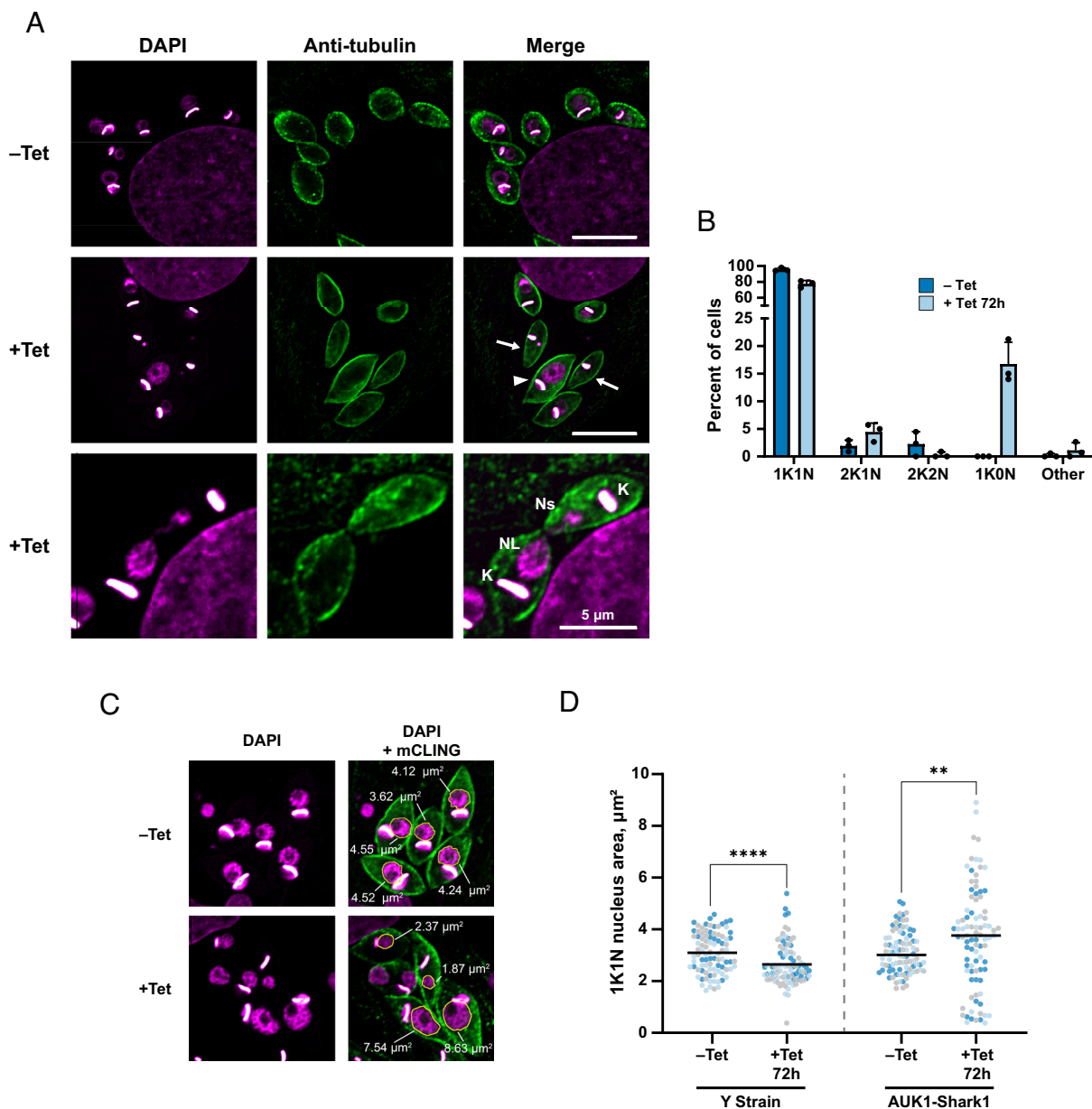


Fig. 7. AUK1 is essential for symmetric mitosis in amastigotes. AUK1-Shark1 tissue culture-derived trypomastigotes were incubated with rat cardiomyocytes (H9C2) adhered to glass coverslips at 37 °C for 24 h. Trypomastigotes were removed and H9C2 cells were incubated ±5 µg/mL Tet for 72 h at 28 °C. Cells were fixed and stained with TAT1 antibody and DAPI for microscopic analysis. (A) Example images of amastigotes in the absence (-Tet, Top row) or presence (+Tet, Bottom two rows) of 5 µg/mL Tet. Arrows indicate trypanosomes without a nucleus. The arrowhead indicates an amastigote with an abnormally large nucleus. Scale bars for Top and Middle rows represent 10 µm. The Bottom row illustrates a 2K2N amastigote undergoing cytokinesis before completion of mitosis. The scale bar represents 5 µm. K = kinetoplast, NL = large nucleus, Ns = small nucleus. (B) The number of K and N per amastigote was determined (N > 100 trypanosomes per replicate in each of three replicates). Other includes 1K2N, 0K1N, and 2K0N cells. (C) Example images of 1K1N nucleus size before and after AUK1 knockdown. The nucleus area in 1K1N amastigotes was measured in ImageJ after manually outlining the nucleus. A gamma correction of 0.7 was applied to the DAPI channel to aid in visualizing the nucleus periphery. The area of each nucleus belonging to a 1K1N amastigote is annotated. (D) Nucleus area measurements for 30 1K1N amastigotes in each of three biological replicates. Data points are color-coded according to the replicate number. Lines indicate the mean nucleus area. A Mann-Whitney *U* test was used to test for a statistical difference between the indicated samples. For Y-strain -Tet vs. +Tet, $P < 1 \times 10^{-4}$; for AUK1-Shark1 -Tet vs. +Tet, $P = 6.9 \times 10^{-3}$.

SHARK system as an important starting point, in future studies, we expect continued refinement of the tagging methodologies and improvement of key aptazyme properties, such as catalytic activity and improved regulation at elevated temperatures.

Since the publication of the TriTryp draft genomes nearly 20 y ago (85), *T. brucei* has enjoyed significant focus and attention, primarily due to the ease of RNAi-based functional studies and screens (85–87), leading to rapid advances in that field. RNAi or gene knockout strategies have been successfully applied to nearly all of *T. brucei*'s protein-coding genes (reviewed in ref. 39). In contrast,

only ~70 of the estimated 12,000 annotated protein-coding genes in *T. cruzi* have been targeted (many unsuccessfully) for deletion, and consequently, our understanding of basic *T. cruzi* biology has progressed at a relatively glacial pace. Until now, the field has been forced to rely on the *inability* to knockout a target gene as evidence of its essentiality. While informative, this strategy has not led to meaningful advances in understanding the specific roles of essential genes in the biology of American trypanosomes.

The development of genetic tools to facilitate the study of *T. cruzi* has taken on increased importance as recent in-depth phylogenetic

comparisons have highlighted significant limitations in using *T. brucei* as the model kinetoplastid. For example, publications analyzing the genomes of both the free-living kinetoplastid *Bodo saltans* (88) and the monoxenous trypanosomatid *Paratrypanosoma confusum* (89) have demonstrated that *T. cruzi* has uniquely retained a number of ancestral genes that were lost in *T. brucei* as it adapted to its unique parasitic niche. Unlike *T. brucei*, *T. cruzi* shares a number of important genetic and morphological characteristics with both monoxenous (single-host) trypanosomatids and free-living kinetoplastids (90), including replicative niches, transmission mechanisms, nutrient uptake, and host–pathogen interactions (reviewed in refs. 91–93). By continuing to dissect the fundamental biology and host adaptations of *T. cruzi*, we can potentially uncover not only effective strategies to combat this deadly parasite but also gain deeper insights into closely related monoxenous trypanosomatids as well as the expansive family of heterotrophic euglenids.

SHARK-mediated knockdown overcomes the roadblock that has remained even after the introduction of CRISPR/Cas9: the lack of a robust method to regulate individual gene expression and functionally characterize essential genes. The three aptazyme versions that we developed are small (~150 base pairs) and offer significant flexibility in experimental design for studying gene function. For example, Shark3 can be used alongside Shark1 for the simultaneous, but independent, regulation of two target genes. Additionally, Shark2 has the potential to provide tight, yet simple, control of transgene expression in *T. cruzi*. Furthermore, our approach does not require the generation of specific parental cell lines and therefore can be applied to any of the major *T. cruzi* strains currently being studied. The SHARK platform offers powerful tools for gene regulation not only for *T. cruzi* but also potentially for other protozoans lacking simple one-step conditional knockdown systems, such as *Leishmania spp.* (87, 94). Our hope is that the introduction and adoption of the SHARK system will enable the field to conduct informative loss-of-function studies in *T. cruzi*, validate potential targets from drug screens, and confirm gene essentiality from any future genome-wide essentiality screens.

1. C. Bern, S. Kjos, M. J. Yabsley, S. P. Montgomery, Trypanosoma cruzi and Chagas' disease in the United States. *Clin. Microbiol. Rev.* **24**, 655–681 (2011), 10.1128/CMR.00005-11.
2. Factsheet: Chagas disease in the Americas for public health workers - PAHO/WHO|Pan American Health Organization, <https://www.paho.org/en/documents/factsheet-chagas-disease-americas-public-health-workers>. 27 January 2022, cited 22 May 2024.
3. P. Nouvellet, E. Dumonteil, S. Gourbrière, The improbable transmission of Trypanosoma cruzi to human: The missing link in the dynamics and control of Chagas disease. *PLoS Negl. Trop. Dis.* **7**, e2505 (2013), 10.1371/journal.pntd.0002505.
4. Z. Brener, Life cycle of Trypanosoma cruzi. *Rev. Inst. Med. Trop. São Paulo* **13**, 171–178 (1971).
5. N. R. Sturm, L. Simpson, Kinetoplast DNA minicircles encode guide RNAs for editing of cytochrome oxidase subunit III mRNA. *Cell* **61**, 879–884 (1990), 10.1016/0092-8674(90)90198-N.
6. G. A. M. Cross, Antigenic variation in trypanosomes. *Am. J. Trop. Med. Hyg.* **26**, 240–244 (1977), 10.4269/ajtmh.1977-26.240.
7. R. E. Sutton, J. C. Boothroyd, Evidence for trans splicing in trypanosomes. *Cell* **47**, 527–535 (1986), 10.1016/0092-8674(86)90617-3.
8. S. Schuster et al., Unexpected plasticity in the life cycle of Trypanosoma brucei. *Elife* **10**, e66028 (2021), 10.7554/elife.66028.
9. K. M. Tyler, D. M. Engman, The life cycle of Trypanosoma cruzi revisited. *Int. J. Parasitol.* **31**, 472–481 (2001), 10.1016/S0020-7519(01)00153-9.
10. N. M. Chasen, I. Coppins, R. D. Etheridge, Identification and localization of the first known proteins of the Trypanosoma cruzi cytosome cytopharynx endocytic complex. *Front. Cell. Infect. Microbiol.* **9**, 445 (2020), 10.3389/fcimb.2019.00445.
11. N. M. Chasen, M. G. Etheridge, R. D. Etheridge, The functional characterization of TcMyoF implicates a family of cytosome-cytopharynx targeted myosins as integral to the endocytic machinery of Trypanosoma cruzi. *mSphere* **5**, e00313-20 (2020), 10.1128/msphere.00313-20.
12. P. C. Campbell, C. L. de Graffenreid, Morphogenesis in Trypanosoma cruzi epimastigotes proceeds via a highly asymmetric cell division. *PLoS Negl. Trop. Dis.* **17**, e0011731 (2023), 10.1371/journal.pntd.0011731.
13. M. S. Bertolini, R. Docampo, MICU1 and MICU2 potentiation of Ca²⁺ uptake by the mitochondrial Ca²⁺ unipporter of Trypanosoma cruzi and its inhibition by Mg²⁺. *Cell Calcium* **107**, 102654 (2022), 10.1016/j.ceca.2022.102654.
14. B. S. Mantilla, C. Azevedo, P. W. Denny, A. Saiardi, R. Docampo, The histidine ammonia lyase of Trypanosoma cruzi is involved in acidocalcisome alkalization and is essential for survival under starvation conditions. *mBio* **12**, e0198121 (2021), 10.1128/mBio.01981-21.
15. F. Díaz-Viraqué, M. L. Chiribao, M. G. Libisch, C. Robello, Genome-wide chromatin interaction map for Trypanosoma cruzi. *Nat. Microbiol.* **8**, 2103–2114 (2023), 10.1038/s41564-023-01483-y.
16. S. M. Ganeshan, A. Falla, S. J. Goldfless, A. S. Nasamu, J. C. Niles, Synthetic RNA–protein modules integrated with native translation mechanisms to control gene expression in malaria parasites. *Nat. Commun.* **7**, 10727 (2016), 10.1038/ncomms10727.
17. C. M. Armstrong, D. E. Goldberg, An FKBP destabilization domain modulates protein levels in Plasmodium falciparum. *Nat. Methods* **4**, 1007–1009 (2007), 10.1038/nmeth1132.
18. M.-H. Huynh, V. B. Carruthers, Tagging of endogenous genes in a Toxoplasma gondii strain lacking Ku80. *Eukaryot. Cell* **8**, 530–539 (2009), 10.1128/ec.00358-08.
19. S. M. Sidki et al., A genome-wide CRISPR screen in Toxoplasma identifies essential apicomplexan genes. *Cell* **166**, 1423–1435.e12 (2016), 10.1016/j.cell.2016.08.019.
20. H. Shi et al., Genetic interference in Trypanosoma brucei by heritable and inducible double-stranded RNA. *RNA* **6**, 1069–1076 (2000), 10.1017/s1355838200000297.
21. H. H. Choudhary, M. G. Nava, B. E. Gartlan, S. Rose, S. Vinayak, A conditional protein degradation system to study essential gene function in Cryptosporidium parvum. *mBio* **11**, e0123120 (2020), 10.1128/mbio.0123120.
22. C. Chagas, Nova tripanozomiae humana: Estudos sobre a morfologia e o ciclo evolutivo do Schizotrypanum cruzi n. gen., n. sp., agente etiológico de nova entidade morbida do homem. *Mem. Inst. Oswaldo Cruz* **1**, 159–218 (1909), 10.1590/S0074-02761909000200008.
23. L. A. M. Trajano-Silva, S. N. Mule, G. Palmisano, "Molecular tools to regulate gene expression in Trypanosoma cruzi" in *Advances in Clinical Chemistry*, G. S. Makowski, Ed. (Elsevier, 2024), pp. 169–190. 10.1016/bs.acc.2024.04.008.
24. F. Callejas-Hernández, A. Rastrojo, C. Poveda, N. Gironès, M. Fresno, Genomic assemblies of newly sequenced Trypanosoma cruzi strains reveal new genomic expansion and greater complexity. *Sci. Rep.* **8**, 14631 (2018), 10.1038/s41598-018-32877-2.
25. S. Alsfeld et al., High-throughput phenotyping using parallel sequencing of RNA interference targets in the African trypanosome. *Genome Res.* **21**, 915–924 (2011), 10.1101/gr.115089.110.
26. W. D. DaRocha, K. Otsu, S. M. R. Teixeira, J. E. Donelson, Tests of cytoplasmic RNA interference (RNAi) and construction of a tetracycline-inducible T7 promoter system in Trypanosoma cruzi. *Mol. Biochem. Parasitol.* **133**, 175–186 (2004), 10.1016/j.molbiopara.2003.10.005.
27. J. Fonager et al., Development of the piggyBac transposable system for *Plasmodium berghei* and its application for random mutagenesis in malaria parasites. *BMC Genomics* **12**, 155 (2011), 10.1186/1471-2164-12-155.

Methods and Materials

Trypanosome and Mammalian Cell culture.

Epimastigote-stage trypanosomes. Insect form *T. cruzi* YC6 (DTU-Tcl) (1, 2) (hereafter referred to as Y-strain) epimastigotes were maintained in early log-phase growth (e.g., <4 × 10⁷/mL) and cultured in liver infusion tryptose (LIT) medium (3, 4) with 15% heat-inactivated fetal bovine serum at 28 °C, as described previously (5). Cell density was determined with a Beckman Coulter Counter. Additional methods describing culture of trypomastigote-stage parasites and mammalian cells can be found in *SI Appendix, SI Methods*.

Assembly and Modification of SHARK Tagging Plasmids. Aptazyme sequences (6) were synthesized as qBlocks (Integrated DNA Technologies) (*SI Appendix, Table S1*, oligos 1 to 8) and incorporated individually into the pMiniTrex-mCherry vector (7) using a HiFi Assembly kit (New England Biolabs, catalog number E5520S) to form the SHARK plasmids (available upon request or via Addgene listed as pMiniTrex-mCherry-Shark1-3). Inactive Tc14 and Theo3 versions containing an A to G mutation near the catalytic core (61) and Tc14 Stem I mutants (U108G, C109A, C110A) were generated by site-directed mutagenesis using primers with single-base mismatches (*SI Appendix, Table S1*; for inactive mutations oligos 9 to 12; for Stem I mutations oligos 13 to 18) with an NEB Q5 site-directed mutagenesis kit (NEB, catalog number E0554S). Additional details can be found in *SI Appendix, SI Methods*.

Detailed methods for trypanosome transfection and cloning, RT-qPCR, western blotting, fluorescence microscopy, proliferation time courses, amastigote proliferation assays, and phenotypic characterization can be found in *SI Appendix, SI Methods*. A list of DNA oligos used in this study may be found in *SI Appendix, Table S1*.

Data, Materials, and Software Availability. All study data are included in the article and/or *SI Appendix*.

ACKNOWLEDGMENTS. We sincerely thank the members of the Center for Tropical and Emerging Global Diseases (CTEGD), the CTEGD Cytometry Shared Resource Laboratory, and the University of Georgia Biomedical Microscopy Core. We wish to thank Dr. Mayara Bertolini for assistance with amastigote studies and helpful discussions. This work was supported by grants provided by the NIH NIAID R01AI163140 and NIGMS R01GM144545 awarded to R.D.E. RH was also partially supported by NIH postdoctoral training grant T32AI060546. We would like to thank Dr. Guocai Zhong for providing additional aptazyme sequences.

28. J. Henriksson *et al.*, Chromosomal localization of seven cloned antigen genes provides evidence of diploidy and further demonstration of karyotype variability in *Trypanosoma cruzi*. *Mol. Biochem. Parasitol.* **42**, 213–223 (1990), 10.1016/0166-6851(90)90164-H.
29. D. Peng, S. P. Kurup, P. Y. Yao, T. A. Minning, R. L. Tarleton, CRISPR-Cas9-mediated single-gene and gene family disruption in *Trypanosoma cruzi*. *mBio* **6**, e02097-14 (2014), 10.1128/mBio.02097-14.
30. A. Nenarokova *et al.*, Causes and effects of loss of classical nonhomologous end joining pathway in parasitic eukaryotes. *mBio* **10**, e01541-19 (2019), 10.1128/mBio.01541-19.
31. N. F. J. van Poppel, J. Welagen, R. F. J. J. Duisters, A. N. Vermeulen, D. Schaap, Tight control of transcription in *Toxoplasma gondii* using an alternative tet repressor. *Int. J. Parasitol.* **36**, 443–452 (2006), 10.1016/j.ijpara.2006.01.005.
32. C. Clayton, Regulation of gene expression in trypanosomatids: Living with polycistronic transcription. *Open Biol.* **9**, 190072 (2019), 10.1098/rsob.190072.
33. N. Lander, Z.-H. Li, S. Niyogi, R. Docampo, CRISPR/Cas9-induced disruption of paraflagellar rod protein 1 and 2 genes in *Trypanosoma cruzi* reveals their role in flagellar attachment. *mBio* **6**, e01012-15 (2015), 10.1128/mBio.01012-15.
34. N. M. El-Sayed *et al.*, The genome sequence of *Trypanosoma cruzi*, etiologic agent of Chagas disease. *Science* **309**, 409–415 (2005).
35. N. G. Jones, C. M. C. Catta-Preta, A. P. C. A. Lima, J. C. Mottram, Genetically validated drug targets in Leishmania: Current knowledge and future prospects. *ACS Infect. Dis.* **4**, 467–477 (2018), 10.1021/acsinfectdis.7b00244.
36. Y. Takagi, Y. Akutsu, M. Doi, K. Furukawa, Utilization of proliferable extracellular amastigotes for transient gene expression, drug sensitivity assay, and CRISPR/Cas9-mediated gene knockout in *Trypanosoma cruzi*. *PLoS Negl. Trop. Dis.* **13**, e0007088 (2019), 10.1371/journal.pntd.0007088.
37. M. Marek *et al.*, Species-selective targeting of pathogens revealed by the atypical structure and active site of *Trypanosoma cruzi* histone deacetylase DAC2. *Cell Rep.* **37**, 110129 (2021), 10.1016/j.celrep.2021.110129.
38. G. F. A. Picchi-Constante *et al.*, Efficient CRISPR-Cas9-mediated genome editing for characterization of essential genes in *Trypanosoma cruzi*. *STAR Protoc.* **3**, 101324 (2022), 10.1016/j.xpro.2022.101324.
39. M. A. Chiurillo, N. Lander, The long and winding road of reverse genetics in *Trypanosoma cruzi*. *Microb. Cell* **8**, 203–207 (2021).
40. Y. F. Ma, L. M. Weiss, H. Huang, A method for rapid regulation of protein expression in *Trypanosoma cruzi*. *Int. J. Parasitol.* **42**, 33–37 (2012), 10.1016/j.ijpara.2011.11.002.
41. Y. Ma, L. M. Weiss, H. Huang, Inducible suicide vector systems for *Trypanosoma cruzi*. *Microbes Infect.* **17**, 440–450 (2015), 10.1016/j.micinf.2015.04.003.
42. N. Lander, T. Cruz-Bustos, R. Docampo, A CRISPR/Cas9-riboswitch-based method for downregulation of gene expression in *Trypanosoma cruzi*. *Front. Cell. Infect. Microbiol.* **10**, 68 (2020), <https://www.frontiersin.org/articles/10.3389/fcimb.2020.00068>.
43. C. Hammann, A. Luptak, J. Perreault, M. de la Peña, The ubiquitous hammerhead ribozyme. *RNA* **18**, 871–885 (2012), 10.1261/rna.031401.111.
44. G. Ferbeyre, J. M. Smith, R. Cedergren, Schistosome satellite DNA encodes active hammerhead ribozymes. *Mol. Cell. Biol.* **18**, 3880–3888 (1998).
45. M. Martick, L. H. Horan, H. F. Noller, W. G. Scott, A discontinuous hammerhead ribozyme embedded in a mammalian messenger RNA. *Nature* **454**, 899–902 (2008), 10.1038/nature07117.
46. G. A. Soukup, R. R. Breaker, Engineering precision RNA molecular switches. *Proc. Natl. Acad. Sci. U.S.A.* **96**, 3584–3589 (1999), 10.1073/pnas.96.7.3584.
47. C. Berens, A. Thain, R. Schroeder, A tetracycline-binding RNA aptamer. *Bioorg. Med. Chem.* **9**, 2549–2556 (2001), 10.1016/S0968-0896(01)00063-3.
48. R. D. Jenison, S. C. Gill, A. Pardi, B. Polisky, High-resolution molecular discrimination by RNA. *Science* **263**, 1425–1429 (1994), 10.1126/science.7510417.
49. K. Beilstein, A. Wittmann, M. Grez, B. Suess, Conditional control of mammalian gene expression by tetracycline-dependent hammerhead ribozymes. *ACS Synth. Biol.* **4**, 526–534 (2015), 10.1021/sb500270h.
50. L. A. Wurmthal, M. Sack, K. Gense, J. S. Hartig, M. Gamerdinger, A tetracycline-dependent ribozyme switch allows conditional induction of gene expression in *Caenorhabditis elegans*. *Nat. Commun.* **10**, 491 (2019), 10.1038/s41467-019-08412-w.
51. G. Zhong, H. Wang, C. C. Bailey, G. Gao, M. Farzan, Rational design of aptazyme riboswitches for efficient control of gene expression in mammalian cells. *Elife* **5**, e18858 (2016), 10.7554/elife.18858.
52. V. Archambault, D. M. Glover, Polo-like kinases: Conservation and divergence in their functions and regulation. *Nat. Rev. Mol. Cell Biol.* **10**, 265–275 (2009), 10.1038/nrm2653.
53. E. Willems *et al.*, The functional diversity of Aurora kinases: A comprehensive review. *Cell Div.* **13**, 7 (2018), 10.1186/s13008-018-0040-6.
54. X. Tu, P. Kumar, Z. Li, C. C. Wang, An Aurora kinase homologue is involved in regulating both mitosis and cytokinesis in *Trypanosoma brucei*. *J. Biol. Chem.* **281**, 9677–9687 (2006), 10.1074/jbc.M511504200.
55. P. Kumar, C. C. Wang, Dissociation of cytokinesis initiation from mitotic control in a eukaryote. *Eukaryot. Cell* **5**, 92–102 (2006), 10.1128/EC.5.1.92-102.2006.
56. T. C. Hammarton, S. Kramer, L. Tetley, M. Boshart, J. C. Mottram, *Trypanosoma brucei* Polo-like kinase is essential for basal body duplication, kDNA segregation and cytokinesis. *Mol. Microbiol.* **65**, 1229–1248 (2007), 10.1111/j.1365-2958.2007.05866.x.
57. N. G. Jones *et al.*, Regulators of *Trypanosoma brucei* cell cycle progression and differentiation identified using a kinome-wide RNAi screen. *PLoS Pathog.* **10**, e1003886 (2014), 10.1371/journal.ppat.1003886.
58. G. Zhong *et al.*, A reversible RNA on-switch that controls gene expression of AAV-delivered therapeutics *in vivo*. *Nat. Biotechnol.* **38**, 169–175 (2020), 10.1038/s41587-019-0357-y.
59. S. Ausländer, P. Ketzer, J. S. Hartig, A ligand-dependent hammerhead ribozyme switch for controlling mammalian gene expression. *Mol. Biosyst.* **6**, 807–814 (2010), 10.1039/B923076A.
60. L. A. Wurmthal, B. Klausner, J. S. Hartig, Highly motif- and organism-dependent effects of naturally occurring hammerhead ribozyme sequences on gene expression. *RNA Biol.* **15**, 231–241 (2018), 10.1080/15476286.2017.1397870.
61. L. Yen *et al.*, Exogenous control of mammalian gene expression through modulation of RNA self-cleavage. *Nature* **431**, 471–476 (2004), 10.1038/nature02844.
62. M. Martick, W. G. Scott, Tertiary contacts distant from the active site prime a ribozyme for catalysis. *Cell* **126**, 309–320 (2006), 10.1016/j.cell.2006.06.036.
63. Z. Li, C. C. Wang, Changing roles of Aurora-B kinase in two life cycle stages of *Trypanosoma brucei*. *Eukaryot. Cell* **5**, 1026–1035 (2006), 10.1128/EC.00129-06.
64. Z. Li, T. Umeyama, Z. Li, C. C. Wang, Polo-like kinase guides cytokinesis in *Trypanosoma brucei* through an indirect means. *Eukaryot. Cell* **9**, 705–716 (2010), 10.1128/EC.00330-09.
65. Z. Li, T. Umeyama, C. C. Wang, The Aurora kinase in *Trypanosoma brucei* plays distinctive roles in metaphase-anaphase transition and cytokinetic initiation. *PLoS Pathog.* **5**, e1000575 (2009), 10.1371/journal.ppat.1000575.
66. J. Wiedeman, K. Mensa-Wilmot, A fixable probe for visualizing flagella and plasma membranes of the African trypanosome. *PLoS One* **13**, e0197541 (2018), 10.1371/journal.pone.0197541.
67. R. E. Jensen, P. T. Englund, Network news: The replication of kinetoplast DNA. *Annu. Rev. Microbiol.* **66**, 473–491 (2012), 10.1146/annurev-micro-092611-150057.
68. R. J. Wheeler, K. Gull, J. D. Sunter, Coordination of the cell cycle in trypanosomes. *Annu. Rev. Microbiol.* **73**, 133–154 (2019), 10.1146/annurev-micro-020518-115617.
69. C. Benz, C. Clucas, J. C. Mottram, Cytokinesis in bloodstream stage *Trypanosoma brucei* requires a family of katanins and spastin. *PLoS One* **7**, e30367 (2012), 10.1371/journal.pone.0030367.
70. S. F. May *et al.*, The *Trypanosoma brucei* AIR9-like protein is cytoskeleton-associated and is required for nucleus positioning and accurate cleavage furrow placement. *Mol. Microbiol.* **84**, 77–92 (2012), 10.1111/j.1365-2958.2012.08008.x.
71. P. D. Andrews, E. Knatko, W. J. Moore, J. R. Swedlow, Mitotic mechanics: The auroras come into view. *Curr. Opin. Cell Biol.* **15**, 672–683 (2003), 10.1016/j.ceb.2003.10.013.
72. M. Fassolari, G. D. Alonso, Aurora kinase protein family in *Trypanosoma cruzi*: Novel role of an AUK-B homologue in kinetoplast replication. *PLoS Negl. Trop. Dis.* **13**, e0007256 (2019), 10.1371/journal.pntd.0007256.
73. T. Sherwin, K. Gull, K. Vickerman, The cell division cycle of *Trypanosoma brucei* brucei: Timing of event markers and cytoskeletal modulations. *Philos. Trans. R. Soc. Lond. B Biol. Sci.* **323**, 573–588 (1989), 10.1098/rstb.1989.0037.
74. D. Ballmer, B. Akiyoshi, Dynamic localization of the chromosomal passenger complex in trypanosomes is controlled by the orphan kinesins KIN-A and KIN-B. *Elife* **13**, RP93522 (2024), 10.7554/elife.93522.
75. K. M. Bonney, D. J. Luthringer, S. A. Kim, N. J. Garg, D. M. Engman, Pathology and pathogenesis of Chagas heart disease. *Annu. Rev. Pathol.* **14**, 421–447 (2019), 10.1146/annurev-pathol-021117-043711.
76. V. Saksmanprone, M. Roychowdhury-Saha, S. Jayasena, A. Khvorova, D. H. Burke, Artificial tertiary motifs stabilize trans-cleaving hammerhead ribozymes under conditions of submillimolar divalent ions and high temperatures. *RNA* **10**, 1916–1924 (2004), 10.1261/ma.7159504.
77. B. W. Kimes, B. L. Brandt, Properties of a clonal muscle cell line from rat heart. *Exp. Cell Res.* **98**, 367–381 (1976), 10.1016/0014-4827(76)90447-X.
78. B. W. Kimes, B. L. Brandt, Characterization of two smooth muscle cell lines from rat thoracic aorta. *Exp. Cell Res.* **98**, 349–366 (1976), 10.1016/0014-4827(76)90446-8.
79. K. N. Ikeda, C. L. deGraffenreid, Polo-like kinase is necessary for flagellum inheritance in *Trypanosoma brucei*. *J. Cell Sci.* **125**, 3173–3184 (2012), 10.1242/jcs.101162.
80. H. Hu, Y. Kurasawa, Q. Zhou, Z. Li, A kinesin-13 family kinesin in *Trypanosoma brucei* regulates cytokinesis and cytoskeleton morphogenesis by promoting microtubule bundling. *PLoS Pathog.* **20**, e1012000 (2024), 10.1371/journal.ppat.1012000.
81. A. Ploubidou, D. R. Robinson, R. C. Docherty, E. O. Ogbadoyi, K. Gull, Evidence for novel cell cycle checkpoints in trypanosomes: Kinetoplast segregation and cytokinesis in the absence of mitosis. *J. Cell Sci.* **112**, 4641–4650 (1999), 10.1242/jcs.112.24.4641.
82. T. C. Hammarton, J. Clark, F. Douglas, M. Boshart, J. C. Mottram, Stage-specific differences in cell cycle control in *Trypanosoma brucei* revealed by RNA interference of a mitotic cyclin. *J. Biol. Chem.* **278**, 22877–22886 (2003), 10.1074/jbc.M300813200.
83. T. C. Hammarton, Cell cycle regulation in *Trypanosoma brucei*. *Mol. Biochem. Parasitol.* **153**, 1–8 (2007), 10.1016/j.molbiopa.2007.01.017.
84. T. Nozaki, G. A. M. Cross, Effects of 3' untranslated and intergenic regions on gene expression in *Trypanosoma cruzi*. *Mol. Biochem. Parasitol.* **75**, 55–67 (1995), 10.1016/0166-6851(95)02512-X.
85. N. M. El-Sayed *et al.*, Comparative genomics of trypanosomatid parasitic protozoa. *Science* **309**, 404–409 (2005), 10.1126/science.1112181.
86. J. C. Kissinger, A tale of three genomes: The kinetoplastids have arrived. *Trends Parasitol.* **22**, 240–243 (2006), 10.1016/j.pt.2006.04.002.
87. N. G. Kolev, C. Tschudi, E. Ullu, RNA interference in protozoan parasites: Achievements and challenges. *Eukaryot. Cell* **10**, 1156–1163 (2011), 10.1128/ec.05114-11.
88. P. Deschamps *et al.*, Phylogenomic analysis of kinetoplastids supports that trypanosomatids arose from within bodonids. *Mol. Biol. Evol.* **28**, 53–58 (2011), 10.1093/molbev/msq289.
89. P. Flegontov *et al.*, Paratrypanosoma is a novel early-branching trypanosomatid. *Curr. Biol.* **23**, 1787–1793 (2013), 10.1016/j.cub.2013.07.045.
90. A. Butenko *et al.*, Reductionist pathways for parasitism in euglenozoans? Expanded datasets provide new insights. *Trends Parasitol.* **37**, 100–116 (2021), 10.1016/j.pt.2020.10.001.
91. S. M. Teixeira, R. M. C. de Paiva, M. M. Kangussu-Marcolino, W. D. Darocha, Trypanosomatid comparative genomics: Contributions to the study of parasite biology and different parasitic diseases. *Genet. Mol. Biol.* **35**, 1–17 (2012), 10.1590/s1415-47572012005000008.
92. A. O. Frolov, A. Y. Kostygov, V. Yurchenko, Development of monoxenous trypanosomatids and phytomonads in insects. *Trends Parasitol.* **37**, 538–551 (2021), 10.1016/j.pt.2021.02.004.
93. R. D. Etheridge, Protozoan phagotrophy from predators to parasites: An overview of the enigmatic cytostome–cytopharynx complex of *Trypanosoma cruzi*. *J. Eukaryot. Microbiol.* **69**, e12896 (2022), 10.1111/jeu.12896.
94. K. A. Robinson, S. M. Beverley, Improvements in transfection efficiency and tests of RNA interference (RNAi) approaches in the protozoan parasite *Leishmania*. *Mol. Biochem. Parasitol.* **128**, 217–228 (2003), 10.1016/S0166-6851(03)00079-3.